10A.6 ATMOSPHERIC PROCESSES ASSOCIATED WITH HEAVY RAINFALL DURING THE EXTRA-TROPICAL TRANSITIONS OF IVAN AND FRANCES

Michael L. Jurewicz, Sr.* and Michael Evans
NOAA/National Weather Service, Binghamton, New York

1. INTRODUCTION

Numerous tropical cyclones impacted the eastern United States during August and September of 2004. During the latter stages of their life cycles, these systems typically produced heavy rainfall over inland areas, which resulted in substantial flooding. In this study, two of these tropical cyclones will be examined: Ivan and Frances. Most of the attention will be focused on Ivan, with relatively brief comparisons to Frances.

Hurricane Ivan made landfall just east of Mobile, Alabama shortly after midnight LDT on September 16, 2004. From Sept. 16-18, Ivan, or the remnants thereof, moved northeastward and eventually exited the Mid-Atlantic coast (Fig. 1a). Excessive rainfall occurred in a band from the central Gulf coast, through the southern and central Appalachians, and into the northeastern United States (Fig. 1b). Hurricane Frances made landfall over east-central Florida during the evening of Sept. 5, 2004. From Sept. 5-10, Frances, or the remnants thereof, curved northward and tracked along the western spine of the Appalachians, then eventually accelerated across northern New England, and into the Canadian Maritime Provinces (Fig. 2a). Excessive rainfall occurred from northern Florida, up the Appalachian Mountain chain and across parts of the Ohio Valley, and ultimately into western New York (Fig. 2b).

In section 2 of this paper, the synoptic-scale setting will be shown from shortly after the time Ivan made landfall on Sept. 16, until extra-tropical transition was well underway over Virginia on Sept. 18. Specific emphasis will be placed on the larger-scale forcing over areas where the heaviest rain fell. In section 3, the mesoscale environments will be examined over the same time period and geographical areas as in the previous section. In order to see how unique the forcing for heavy precipitation was with Ivan, comparisons will be made to the forcing associated with Frances. Also, the forcing mechanisms shown in this study will be compared to those associated with a major winter storm. Lastly, a summary will be given in section 4. Within the summary section, a schematic is presented, which ties together important ingredients for heavy rainfall identified in previous research of extra-tropical transitioning cyclones, with those noted in this study. This conceptual model

* *Address for correspondence*: Michael L. Jurewicz, Sr., National Weather Service, 32 Dawes Drive, Johnson City, NY 13790.
E-mail: Michael.Jurewicz@noaa.gov

will be compared and contrasted to methodologies typically used to perform winter storm diagnostics.

2. SYNOPTIC OVERVIEW OF IVAN

At 1200 UTC on Sept. 16 (1200/16, about six hours after landfall), the center of circulation of hurricane Ivan was over southern Alabama. Ivan was still well separated from the main belt of northern-stream westerlies. Composite radar imagery (not shown) showed that Ivan's heavy rain bands remained concentric in nature and tightly clustered around the system.

Ivan moved slowly northward during the day on the 16th. By evening (0000/17), the circulation center was over northern Alabama (not shown). Although Ivan was still positioned south of the westerlies at this point, its continued northward track raised the likelihood of increased interaction with the mid-latitude westerlies, located just to the north. In fact, favorable upper-tropospheric jet dynamics (not shown) were already aiding large-scale lift over the Tennessee Valley at this time, leading to an expansion of the heavy rain shield northward into this region. The strong correlation between heavy rainfall and the equatorward entrance-region of strengthening upper-tropospheric jet streaks, during the extra-tropical transition phase of tropical cyclones, has been well documented in previous research (Atallah and Bosart 2003; Hart and Evans 2003; Thorncroft and Jones 2000; Sinclair 1993).

During the overnight period, from the evening hours of the 16th into the early morning of the 17th, Ivan's circulation center edged northeastward, reaching eastern Tennessee by 1200/17 (not shown). Ivan had begun to take on extra-tropical characteristics by this time, as evidenced by several factors. Within the lower to middle-troposphere, the thermal characteristics of the system were transitioning from a warm-core structure to a baroclinic structure (not shown). In the lower-troposphere, the circulation center of Ivan was approaching both a decelerating frontal boundary at the surface and tightening temperature gradient at 925 hPa. The main vorticity center had started to separate itself from maxima in the thickness fields, heralding the first stages of metamorphosis towards a colder-core system. Tracking the migration of the vorticity maxima, from the vicinity of warm-core thickness values towards gradient zones in the tropospheric thickness fields, has been a technique used to assess the progression of the extra-tropical transition process in several recently studied, high profile cyclones, such as Floyd in 1999, Opal in 1995, and Agnes in 1972 (Attalah and Bosart 2003; Bosart et al. 2000; Bosart and Dean 1991; Bosart and Carr 1978). Additionally, the primary potential vorticity (PV) center associated with Ivan was beginning to stretch vertically (not shown), and also upshear towards incoming short-wave energy in the northern-stream branch of the westerlies. Similar PV reorientation has been observed previously when tropical cyclones began to interact with mid-latitude troughs (Atallah and Bosart 2003; Hart 2003; Browning et al. 2000; Klein et al. 2000; Bevin 1997).

Between 0000/17 and 1200/17, the strength of the upper-tropospheric jet streak over the Great Lakes region increased markedly. Previous studies have also observed this tendency for strengthening of the upper-tropospheric

jet poleward of transitioning tropical cyclones; and have speculated that this was due primarily to enhanced upper-tropospheric outflow from the cyclone toward the jet (Attalah and Bosart 2003; Colle 2003; Sinclair 2002; Sinclair, 1993). As this relatively warm outflow evacuates from the remnant tropical circulation, upper-tropospheric ridging is promoted poleward of the cyclone. This ridging tightens the height gradient south of the westerlies, leading to increased shear, and a more pronounced jet streak.

As the upper-tropospheric jet intensified between 0000/17 and 1200/17, associated divergence within its right-entrance region also increased (not shown). The heavy rain shield continued to expand northward into the area of strongest upper-tropospheric divergence. The area of maximum divergence continued to propagate towards the north-northeast, just ahead of Ivan's main circulation center. These motions suggest a coupling between Ivan and the region of maximum upper-tropospheric divergence, perhaps substantiating the link between Ivan's outflow and the magnitude of the jet core, described earlier in this section. Attalah and Bosart (2003) elaborate on a similar coupling between Floyd and an intense equatorward jet-entrance region to the north in Sept. of 1999.

Ivan began to track more eastward during the day on Sept. 17. By early evening (0000/18), its circulation center was near the border of southwestern Virginia and western North Carolina (Fig. 3). The system continued to become increasingly baroclinic, especially in the lower-troposphere. Interaction with the surface boundary, along with tightening temperature gradients in the 925-850 hPa layer, just north of the surface front, were quite evident by 0000/18 (Fig. 3a). The mid-tropospheric vorticity maximum had become embedded within the 1000-500 hPa thickness gradient (Fig. 3b), indicating that a change in thermal structure towards a cold-core system was well underway (Attalah and Bosart 2003; Bosart et al. 2000; Thorncroft and Jones 2000). Meanwhile, the PV maximum associated with Ivan continued to stretch vertically. The primary PV maximum, originally located in the lower-troposphere (800-600 hPa) while Ivan had retained its tropical characteristics, was now located in the upper-troposphere, (300 hPa and above) as energy from a mid-latitude trough merged into the system (Fig. 3c).

As Ivan continued to move eastward between 1200/17 and 0000/18, the pronounced upper-tropospheric jet (around 150 kt) and area of divergence to its north did likewise (Fig. 3d), indicating a continued coupling between Ivan and the maximum upper-tropospheric divergence. The area of heaviest rainfall also moved eastward from the Ohio Valley into Pennsylvania and southern New York State by 0000/18 (Fig. 4).

During the overnight period and into the early morning (0000/18 to 1200/18), Ivan continued to track eastward, reaching the Virginia coast by 1200/18. In the lower-troposphere, the transition to a baroclinic system was nearly complete. At the surface, Ivan had taken on a frontal-wave structure, while very strong 925-850 hPa temperature gradients and thermal advections were in place. The primary mid-tropospheric vorticity maxima remained solidly within the gradient of tropospheric thickness values, indicating that its former warm-core structure had completely broken down. Additionally,

Ivan's PV core was still stretched out in the vertical towards a maximum at and above 300 hPa (not shown), indicating the linkage to an upper-tropospheric short-wave.

As Ivan's circulation center moved eastward across Virginia between 0000/18 and 1200/18, the well developed entrance-region of the upper-tropospheric jet continued its corresponding eastward progression. Radar imagery (not shown) showed that the heaviest rainfall had shifted into eastern Pennsylvania and eastern New York by 1200/18, well collocated with the area of most intense upper-tropospheric divergence.

During the day on the 18th, the steadier rainfall shifted off the coast from New Jersey to southern New England. Some weakening of the rainfall intensity was noted during this time frame, as the larger-scale forcing mechanics began to disorganize and become less intense.

3. MESOSCALE SETTINGS

At 0000/17 (12 to 18 hours after landfall), radar mosaics (not shown) showed that the most concentrated rainfall associated with Ivan was across northern Alabama and eastern Tennessee. As mentioned in section 2, an upper-tropospheric divergence maximum had developed over this area, within the equatorward entrance-region of a strengthening jet streak to the north (not shown). In response, a thermally-direct ageostrophic circulation was in place, leading to the development of an enhanced lower-tropospheric southeasterly jet (Blanchard et al. 1998; Hamilton et al. 1998).

Tropical air was transported northward by the lower-tropospheric jet. As this warm, moist air mass interacted with somewhat cooler, drier air over the Tennessee Valley, temperature and moisture gradients developed, which helped to increase lower-tropospheric frontogenesis. An initialized model cross-section (not shown), from the North American Model (NAM), showed that the best combination of lower-tropospheric frontogenesis and elevated gravitational instability existed across eastern Tennessee at 0000/17, well collocated with the heaviest rain bands.

The roles of frontogenetic forcing and moist symmetric instability in the production of heavy precipitation, as well as their operational diagnoses, have been well studied (Schultz and Schumacher 1999; Emanuel 1985; Hsie et al. 1984). From the 1990's through about 2002, most of the attention in the literature was given to cold-season events that involved locally heavy snowfall (Novak et al. 2002; Nicosia and Grumm 1999; Martin 1998). Since 2002, however, studies that have examined the contributions of frontal-scale forcing towards heavy rainfall, during the extra-tropical transition process, have become more common (Colle 2003; Dickinson and Bosart 2002).

Regarding Ivan's evolution during the following 36 hours (from after 0000/17 to 1200/18), as stated in section 2, a consistent trend towards increased baroclinicity was noted, especially in the lower-troposphere. A well developed lower-tropospheric jet continued to pump tropical air northward and over a stationary surface front, which resulted in strong equivalent potential temperature (θe) advection and convergence during this time frame (Fig. 5). The resultant strong temperature gradient, along with deformation,

resulted in maxima of 2-D (Peterson) frontogenesis in the 925-850 hPa layer (Fig. 6), well to the north of Ivan's circulation center, and just north of the aforementioned surface boundary. Figure 6 also indicates that a heavy stratiform rain band formed in an area where strong lower-tropospheric frontogenesis was collocated with negative equivalent potential vorticity (EPV; with the real-wind as opposed to the geostrophic wind used in the calculation), indicating that the environment near the frontogenesis was susceptible to slantwise (and possibly even vertical) convection. An examination of the vertical distribution of θe (not shown) indicated the presence of conditional instability across a portion of this negative EPV region. Meanwhile, convective "feeder bands," that were more isolated in nature, were primarily relegated to the southern and eastern quadrants of Ivan's sphere of influence (not shown). These "feeder bands" resided in environments characterized by deep negative EPV and conditional instability, but weak lower-tropospheric thermal gradients, and thus minimal frontogenetic forcing.

Similar atmospheric processes were at play, where the heaviest rain fell, during the extra-tropical transition phase of tropical cyclone Frances. For instance, radar imagery (not shown) from the Pittsburgh, PA (KPBZ) WSR-88D at 0000 UTC, Sept. 9 (0000/9), showed intense, smaller-scale rain bands over western Pennsylvania, within a much larger precipitation shield, and also well northward of the main circulation center.

Data from the NAM analysis (not shown) indicated that an upper-tropospheric jet entrance-region was also in place across western Pennsylvania at 0000/9. A thermally- direct ageostrophic circulation was once again present, in response to the enhanced upper-tropospheric jet to the north, which forced the development of a lower-tropospheric southeasterly jet (Blanchard et al. 1998; Hamilton et al. 1998). The nose of this lower-tropospheric jet was pointed towards western Pennsylvania, which ultimately resulted in strong thermal and moisture advections, and a resulting strong gradient, due to the influx of tropical air and its interaction with a lower theta-e air mass to the north.

The tight temperature gradient associated with this environment was a key contributor towards a strong maximum of lower-tropospheric frontogenesis. From a cross-sectional perspective (Fig. 7), a sloped frontal boundary was evident with Frances, similar to the boundary observed with Ivan. The aforementioned heavy rain bands, across western Pennsylvania, were positioned in a region where a maximum of lower-tropospheric frontogenesis was located just below an area of negative EPV. As was the case with Ivan, an examination of the vertical distribution of θe indicated the presence of conditional instability across a portion of this negative EPV region. Convective "feeder bands," located farther to the southeast over Virginia at this time, resided in a very unstable environment, but also one where frontal-scale forcing was much shallower in nature. These findings are generally consistent with those uncovered during the investigation of Ivan. The frontal-scale structures of Ivan and Frances also showed many similarities to the environment associated with tropical cyclone Floyd, during its extra-tropical transition over the northeastern United States in Sept. of

1999 (Attalah and Bosart 2003; Colle 2003).

As outlined earlier in this section, the same atmospheric components and processes (jet induced ageostrophic circulations, strong frontogenesis, and elevated conditional instability, all in the presence of deep saturation) that triggered the heaviest rainfall during Ivan's and Frances' extra-tropical transitions, have also been commonly observed with banded heavy snowfall (Novak et al. 2004; Clark et al. 2002). In order to provide a direct comparison, data will be shown from a recent significant winter storm.

On January 21-24, 2005, heavy snow and ice affected a large portion of the central and eastern United States, from the Midwest, all the way to the Mid-Atlantic and Northeastern states. The greatest impacts from this storm were felt over southern New England, from late in the evening on Jan. 22 into the afternoon of Jan. 23, when blizzard conditions prevailed. Snowfall totals of 2 to 3 feet were common across southern and eastern Massachusetts, as well as Rhode Island. Heavy snowfall was also driven by strong winds, that locally reached hurricane force near the coast (Stephens 2005).

At 1200 UTC, Jan. 23, (1200/23) moderate to heavy snow was falling over much of southern and eastern New England (Fig. 8). A particularly heavy snow band was situated from the Gulf of Maine, to the northern Massachusetts coast, then back across central Massachusetts and northern Connecticut. A favorable upper-tropospheric jet configuration was set up along the east coast of the United States, with a coupled jet core structure and strong upper-tropospheric divergence from southeastern New England to the offshore waters (not shown). In response to the upper tropospheric jets, a thermally-direct ageostrophic circulation induced the development of an enhanced easterly lower-tropospheric jet, directed at the New England coast (Blanchard et al. 1998; Hamilton et al. 1998).

As Atlantic inflow, via the above mentioned lower-tropospheric jet, interacted with a dome of Arctic air just inland, thermal and moisture gradients tightened substantially. This scenario resulted in the formation of a strong, vertically sloped frontal boundary across southern and eastern New England. Comparing cross-sectional model data (Fig. 9) of the frontal-scale structure to a regional radar mosaic (Fig. 8) shows very good correlation between the most intense banded feature with enhanced reflectivity, strong frontogenesis, and reduced stability aloft. Snowfall rates of 5" or more per hour were associated with this snow band, over parts of eastern Massachusetts, between 0900 UTC and 1500 UTC, Jan. 23 (Stephens 2005).

4. SUMMARY

The atmospheric processes that coincided with heavy stratiform rainfall over the eastern United States during the extra-tropical transitions of Ivan and Frances in Sept. of 2004 were examined. Between 1200/16 and 1200/18, Ivan tracked northward from the Gulf coast into the Tennessee Valley, then eastward to the Virginia coast (Fig. 1a). During this time, Ivan's loss of tropical characteristics was shown primarily in two ways. First, the thermal structure of the system transitioned from a warm-core nature to one of increased baroclinicity. This was evidenced by tightening lower-tropospheric

temperature gradients near and north of the circulation center (refer back to Fig. 3a). Also, the primary mid-tropospheric vorticity maxima migrated from their positions near the warmest thicknesses, to ones embedded within a gradient of tropospheric thickness values (Fig. 3b). Second, Ivan began to interact with energy from an incoming mid-latitude trough. This was shown through a reorientation of Ivan's PV center, both upward vertically and upshear horizontally, as the northern-stream short-wave and Ivan merged together (Fig. 3c).

A strong upper-tropospheric jet streak developed well to the north of Ivan's main circulation center. The magnitude of the jet core was enhanced, as relatively warm middle to upper-tropospheric outflow from Ivan tightened the height gradient over areas to the north, and thus increased shear. Pronounced upper-tropospheric divergence formed within the equatorward entrance region of the above mentioned jet streak (Fig. 3d). In response to this divergence, a thermally-direct ageostrophic circulation developed, which resulted in an enhanced southeasterly flow in the lower-troposphere (Blanchard et al. 1998; Hamilton et al. 1998).

The lower-tropospheric jet transported tropical air northward. Meanwhile, much cooler, drier air was pushing southward from Ontario and the northern Great Lakes region. Interaction between these two air masses set up a tight thermal gradient to the north of Ivan's circulation center, which led to enhanced frontogenesis. The associated sloping frontal zone was characterized by frontogenesis sloping upward towards the northwest. The presence of conditional instability or reduced stability, just above this sloped frontal zone, acted to increase the vigor of the ageostrophic frontal circulation in these areas, and thus intensify slantwise ascent (Fig. 6) (Schultz and Schumacher 1999; Emanuel 1985). It was consistently in these places, where frontal-scale forcing was maximized well north of the main circulation center, that the heaviest stratiform rainfall (including some embedded and intense banded development) occurred during the extra-tropical transition phases of both Ivan and Frances. Locally excessive rainfall amounts (Figs. 1b and 2b) from the southern Appalachians and the Ohio Valley, into the northeastern United States, resulted in several fatalities, as well as millions of dollars in damages to infrastructure and personal property.

Many common synoptic and frontal-scale elements were also noted between those observed in this study, and ones identified in previous research of Floyd's extra-tropical transition back in 1999 (Attalah and Bosart 2003; Colle 2003) In addition, some interesting similarities (namely, the coexistence of heavy stratiform precipitation bands, strong frontogenesis, and conditional instability or reduced stability aloft) are noted between the environments associated with these tropical systems, and the environment associated with a significant winter storm over southeastern New England in January of 2005. There were also subtle differences. There was a shallower depth of conditional instability or reduced stability for the winter case, as opposed to the tropical systems. Also, the fronts were more steeply sloped in the extra-tropical transition cases, when compared to the winter storm event.

A schematic was constructed that highlights the most important forcing

mechanisms that were responsible for heavy stratiform rainfall in this study (Fig. 10). Many of these same atmospheric components (jet induced ageostrophic circulations, strong frontogenesis, and elevated conditional instability, all in the presence of deep saturation) have been identified as prime ingredients for heavy, banded precipitation associated with significant cold-season cyclones (Novak et al. 2004; Clark et al. 2002; Novak et al. 2002; Nicosia and Grumm 1999; Martin 1998). In the schematic (Fig. 10), an attempt is made to approximate the thermal structure, with regards to the height of the freezing level. Analyses of both the temperature structure and depth of saturation in cross-sectional formats allow forecasters to assess warm cloud depths (WCD) for areas of concern. With both Ivan and Frances, WCD's were more than adequate to enhance rainfall efficiency in the regions of heavy stratiform precipitation, given the ingest of warm, moist air into the mid-troposphere.

Prior research has correlated WCD layers of 3-4 km, or more, with dominant "warm rain" or coalescence processes, and significantly enhanced rainfall rates/efficiency (Davis 2001; Doswell et al. 1996). In this way, the WCD could be considered a modulating factor for potential heavy rainfall, when other favorable ingredients are in place. To provide a comparison to potential heavy snow situations, the modulating effects of the WCD would be analogous to those of favorable dendrite growth regions (temperatures between -12°C and -18°C, in the presence of saturated conditions and upward motion) (Roebber et al. 2003; Power et al. 1964).

Plans for future work include research on other recent extra-tropical transitioning cyclones over the eastern United States. A goal of these studies would be to create a more in-depth conceptual model of the synoptic and frontal-scale processes typically associated with heavy stratiform rainfall.

5. REFERENCES

Attalah, E.H. and L.F. Bosart, 2003: The Extratropical Transition and Precipitation Distribution of Hurricane Floyd (1999). *Mon. Wea. Rev.*, **131,** 1063-1081.

Bevin, J.L. II, 1997: A Study of Three "Hybrid" Storms. Preprints, *22nd Conf. on Hurricanes and Tropical Meteorology*, Fort Collins, CO, Amer. Meteor. Soc., 645-646.

Blanchard, D.O., W.R. Cotton, and J.M. Brown, 1998: Mesoscale circulation Growth under Conditions of Weak Inertial Instability. *Mon. Wea. Rev.*, **126**, 118-140.

Bosart, L.F., C.S. Velden, W.E. Bracken, J. Molinari, and P.G. Black, 2000: Environmental Influences on the Rapid Intensification of Hurricane Opal (1995) over the Gulf of Mexico. *Mon. Wea. Rev.*, **128**, 322-352.

Bosart, L.F. and D.B. Dean, 1991: The Agnes Rainstorm of June 1972: Surface Feature Evolution Culminating in Inland Storm Redevelopment. *Wea. Forecasting,* **6**, 515-537.

Bosart, L.F. and F.H. Carr, 1978: A Case Study of Excessive Rainfall Centered around Wellsville, New York, 20-21 June, 1972. *Mon. Wea. Rev.*, **106**, 348-362.

Browning, K.A., A.J. Thorpe, A. Montani, D. Parsons, M. Griffiths, P. Panagi, and E.M. Dicks, 2000: Interactions of Tropopause

Depressions with an Ex-tropical Cyclone and Sensitivity of Forecasts to Analysis Errors. Mon. Wea. Rev., **128**, 2734-2755.

Clark, J.H., R.P. James, and R.H. Grumm, 2002: A Re-examination of the Mechanisms Responsible for Banded Precipitation. *Mon. Wea. Rev.*, **130**, 3074-3086.

Colle, B.A., 2003: Numerical Simulations of the Extratropical Transition of Floyd (1999): Structural Evolution and Responsible Mechanisms for the Heavy Rainfall over the Northeast United States. *Mon. Wea. Rev.* **131**, 2905-2926.

Davis, Robert S., 2001: Flash Flood Forecast and Detection Methods. Severe Convective Storms, Meteorological Monographs, 28, Amer. Meteor. Soc.

Dickinson, M.J. and Bosart, L.F., 2002: An Examination of the Mesoscale Structure Associated with the Extratropical Transition of Hurricane Agnes (1972). Preprints, *19th Conf. on Weather Analysis and Forecasting*, San Antonio, TX, Amer. Meteor. Soc., CD-ROM, p. 10.7.

Doswell, C.A. III, H.E. Brooks, and R.A. Maddox, 1996: Flash Flood Forecasting: An Ingredients-based Methodology. *Wea. Forecasting,* **11**, 560-581.

Emanuel, K.A., 1985: Frontal Circulations in the Presence of Small Moist Symmetric Instability. *J. Atmos. Sci.,* **42**, 1062-1071.

Hamilton, D.W., Y. Lin, R.P. Weglarz, and M.L. Kaplan, 1998: Jetlet Formation from Diabatic Forcing with Applications to the 1994 Palm Sunday Tornado Outbreak. *Mon. Wea. Rev.*, **126**, 2061-2089.

Hart, R.E. and J.L. Evans, 2003: Objective Indicators of the Life Cycle Evolution of Extratropical Transition for Atlantic Tropical Cyclones. *Mon. Wea. Rev.*, **131**, 745-761.

Hart, R.E., 2003: A Cyclone Phase Space Derived from Thermal Wind and Thermal Assymetry. *Mon. Wea. Rev.*, **131**, 585-616.

Hsie, E.Y., R.A. Anthes, and D. Keyser, 1984: Numerical Simulation of Frontogenesis in a Moist Atmosphere. *J. Atmos. Sci.*, **41**, 2581-2594.

Klein, P.M., P.A. Harr, and R.L. Elsberry, 2000: Extra-tropical Transition of Western North Pacific Tropical Cyclones: An Overview and Conceptual Model of the Transformation Stage. *Wea. Forecasting,* **15**, 373-396.

Martin, J.E., 1998: The Structure and Evolution of a Continental Winter Cyclone. Part II: Frontal Forcing of an Extreme Snow Event. *Mon. Wea. Rev.*, **126**, 329-348.

Nicosia, D.J. and R.H. Grumm, 1999: Mesoscale Band Formation in Three Major Northeastern United States Snowstorms. *Wea. Forecasting,* **14,** 346-368.

Novak, D.R., L.F. Bosart, D. Keyser, and J.S. Waldstreicher, 2004: An Observational Study of Cold Season-Banded Precipitation in Northeast U.S. Cyclones. *Wea. Forecasting*, **19**, 993-1010.

Novak, D.R., L.F. Bosart, D. Keyser, and J.S. Waldstreicher, 2002: A Climatological and Composite Study of Cold Season-Banded Precipitation in the Northeast United States. Preprints, *19th Conf. on Weather Analysis and Forecasting,* San Antonio, TX,

Amer. Meteor. Soc., CD-ROM, p. 6.5.

Power, B.A., P.W. Summers, and J. d'Auignon, 1964: Snow Crystal Forms and Riming Effects as Related to Snowfall Density and General Storm Conditions. *J. Atmos. Sci.*, **21**, 300-305.

Roebber, P.J., S.L. Breuning, D.M. Schultz, and J.V. Cortinas, Jr., 2003: Improving Snowfall Forecasting by Diagnosing Snow Density. *Wea. Forecasting,* **18**, 264-287.

Schultz, D.M. and P.N. Schumacher, 1999: The Use and Misuse of Conditional Symmetric Instability. *Mon. Wea. Rev.*, **127**, 2709-2732.

Sinclair, M.R., 2002: Extratropical Transition of Southwest Pacific Tropical Cyclones. Part I: Climatology and Mean Structure Changes. *Mon. Wea. Rev.*, **130**, 590-609.

Sinclair, M.R., 1993: Synoptic-scale Diagnosis of the Extratropical Transition of a Southwest Pacific Tropical Cyclone. *Mon. Wea. Rev.*, **121**, 941-960.

Stephens, S., cited 1005: Climate of 2005: Global Hazards and Significant Events. National Climatic Data Center. 5 April 2005, <http:www.ncdc.noaa.gov/oa/climate/research/2005/jan/hazards.html#WINTER>

Thorncroft, C. and S.C. Jones, 2000: The Extratropical Transitions of Hurricanes Felix and Iris in 1995. *Mon. Wea. Rev.*, **128**, 947-972.

FIGURES

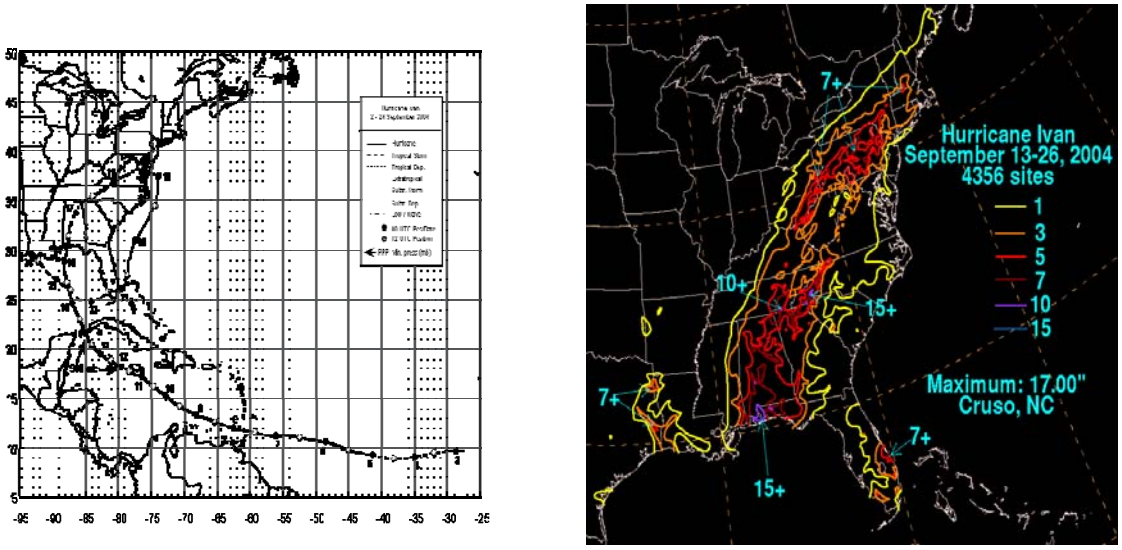

(a) (b)

Figure 1. NOAA National Weather Service, Tropical Prediction Center (TPC) plots of: a) The track of tropical cyclone Ivan, and b) Observed rainfall associated with Ivan.

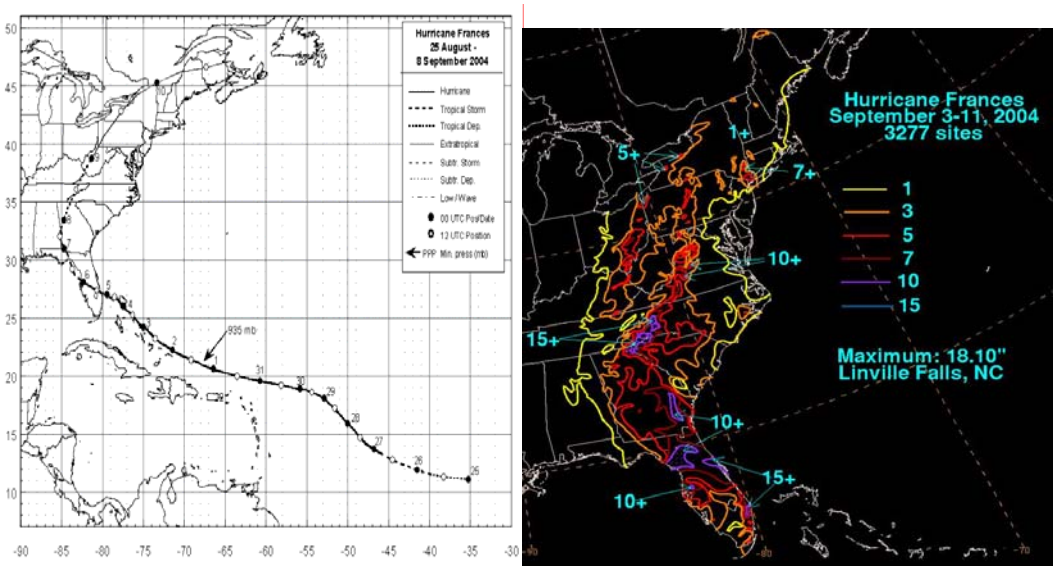

(a) (b)

Figure 2. TPC plots of: a) The track of tropical cyclone Frances, and b) Observed rainfall associated with Frances.

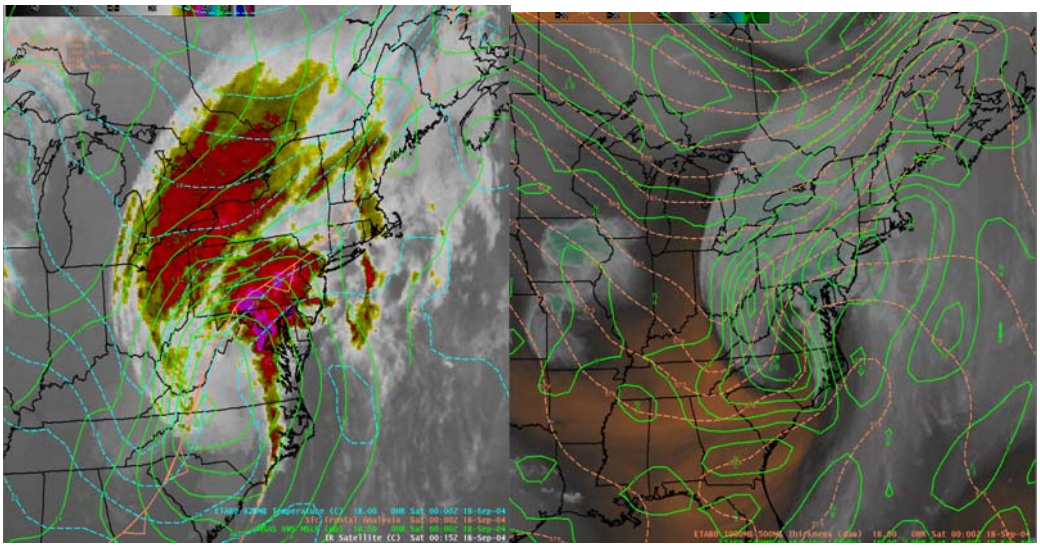

(a) (b)

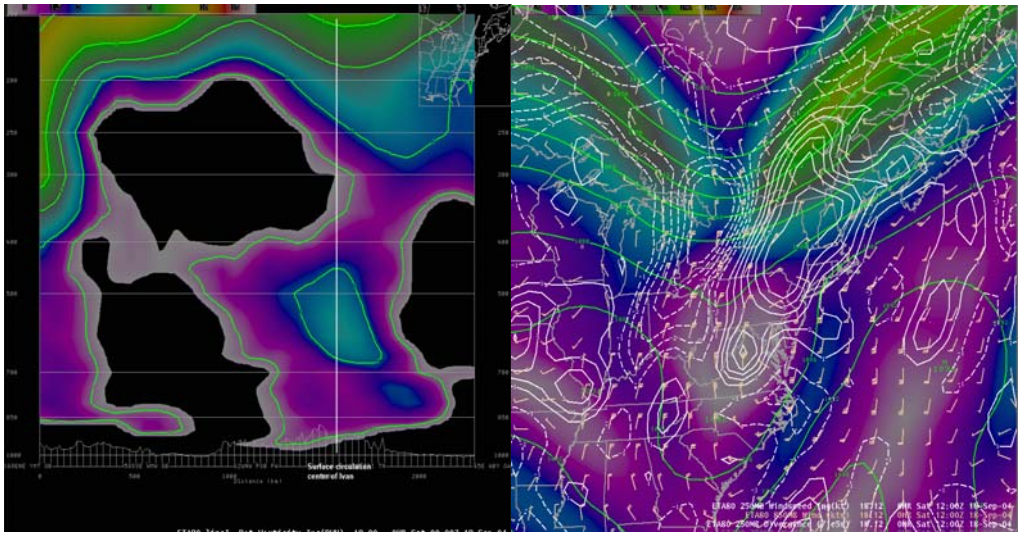

(c) (d)

Figure 3. North American Model (NAM) analyses, valid at 0000/18 of: a) Mean sea-level pressure (MSLP) (solid green, hPa) and 925 hPa temperatures (blue dashed, ºC), along with surface frontal positions (orange), superimposed on infrared satellite imagery, b) 500 hPa vorticity (solid green, 10^{-5} s^{-1}) and 1000-500 hPa thicknesses (dashed orange, dm), superimposed on water vapor imagery, c) A cross-section (axis drawn from Georgia to Quebec) of PV (contoured every 2.0 PVU (10^{-6} ºK kg^{-1} m^2 s^{-1}) starting at 0.0 PVU, with shading also provided), and d) 250 hPa heights (solid green, dm), divergence (solid white, s^{-1}), and winds (shaded, kt), as well as 850 hPa winds (tan wind barbs). The approximate location of Ivan's surface circulation center is noted along the x-axis of Fig. 3c.

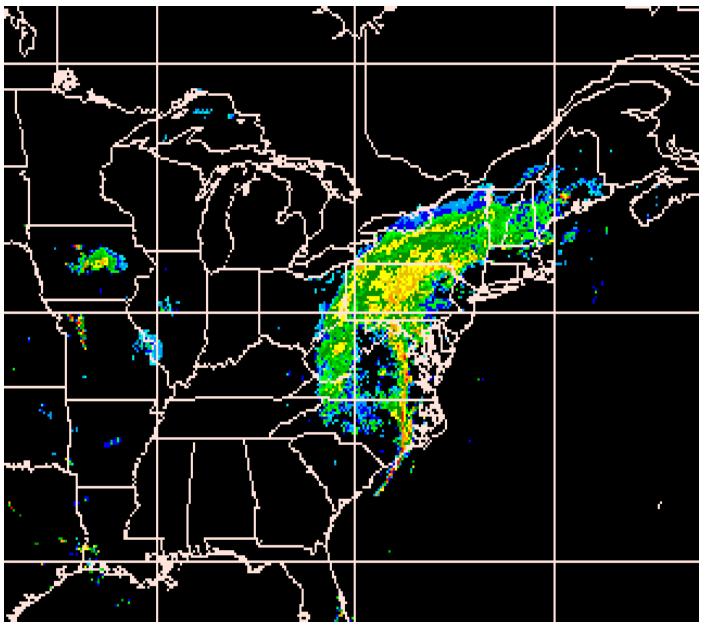

Figure 4. A 2-km resolution WSR-88D mosaic of 0.5° reflectivity (CONUS-scale), valid at 0000/18.

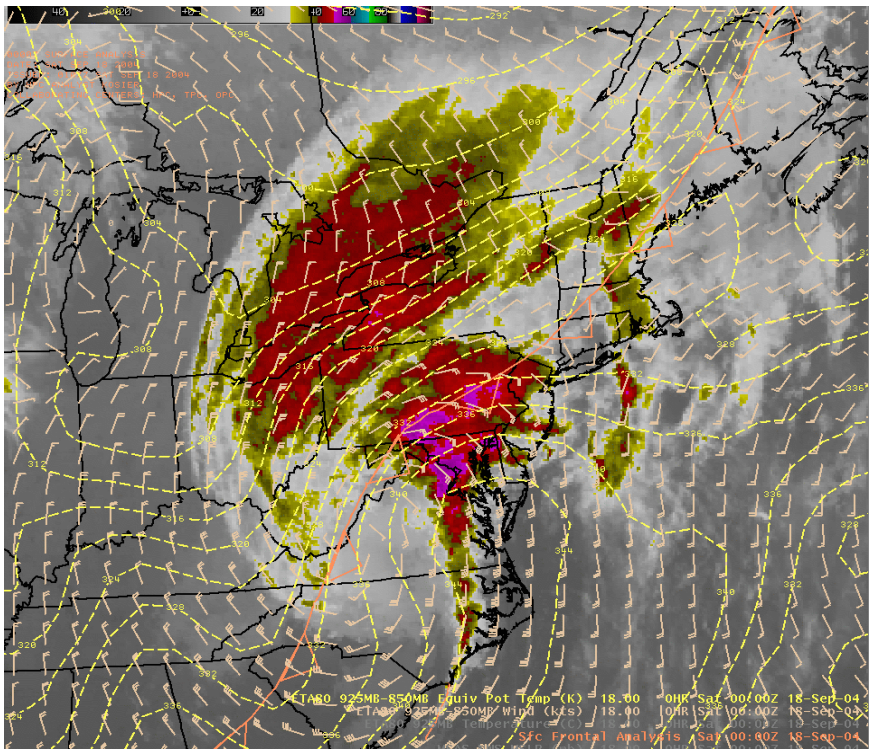

Figure 5. NAM analysis of 925-850 hPa mean layer θe (dashed yellow, ºK) and winds (tan wind barbs, kt), along with surface frontal analysis, all valid at 0000/18.

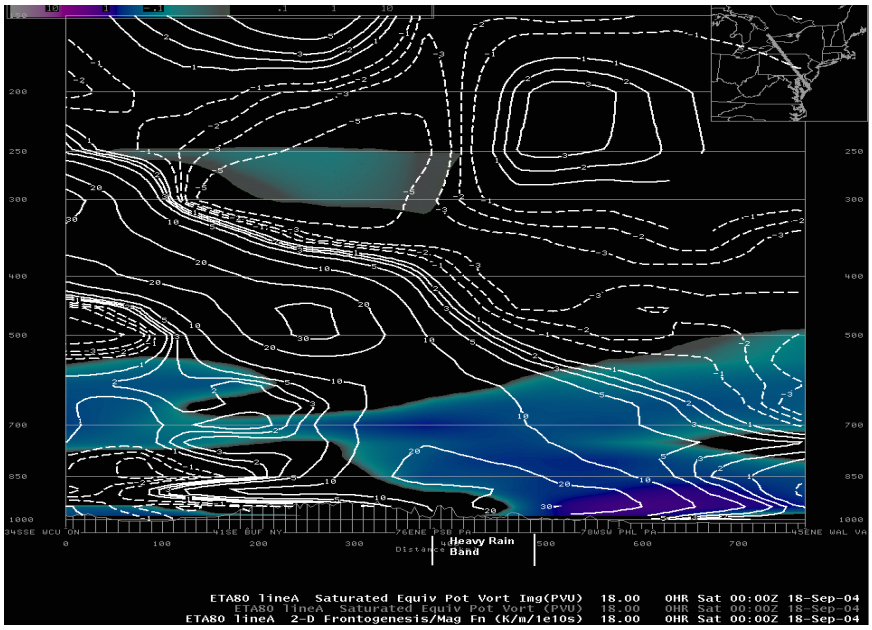

Figure 6. NAM initialized cross-section of 2-D frontogenesis (solid white, °K (100 km)$^{-1}$ (3h)$^{-1}$) and saturated equivalent potential vorticity (EPV) (negative and weakly positive (0.0 to 0.1 PVU) values shaded, 10^{-7} °K (Pa s)$^{-1}$), valid at 0000/18. The cross-sectional axis was drawn from southeastern Maryland to southern Ontario. The approximate location of stratiform heavy rain bands are noted along the x-axis.

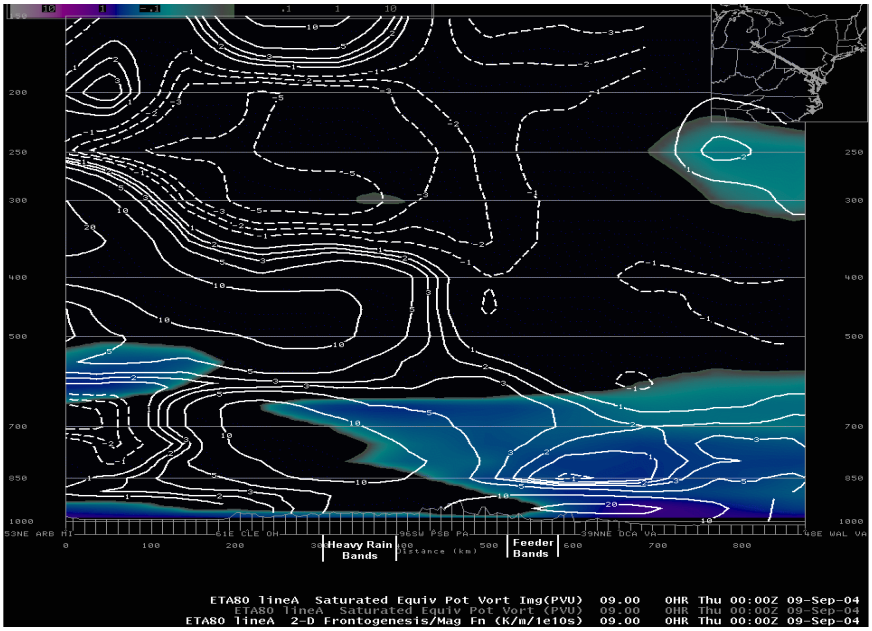

Figure 7. NAM initialized cross-section of 2-D frontogenesis (solid white, °K (100 km)$^{-1}$ (3h)$^{-1}$) and saturated EPV (negative and weakly positive (0.0 to 0.1 PVU) values shaded, 10^{-7} °K (Pa s)$^{-1}$), valid at 0000/9. The cross-sectional axis was drawn from southeastern Maryland to Michigan. The approximate locations of stratiform heavy rain bands and convective feeder bands are noted along the x-axis.

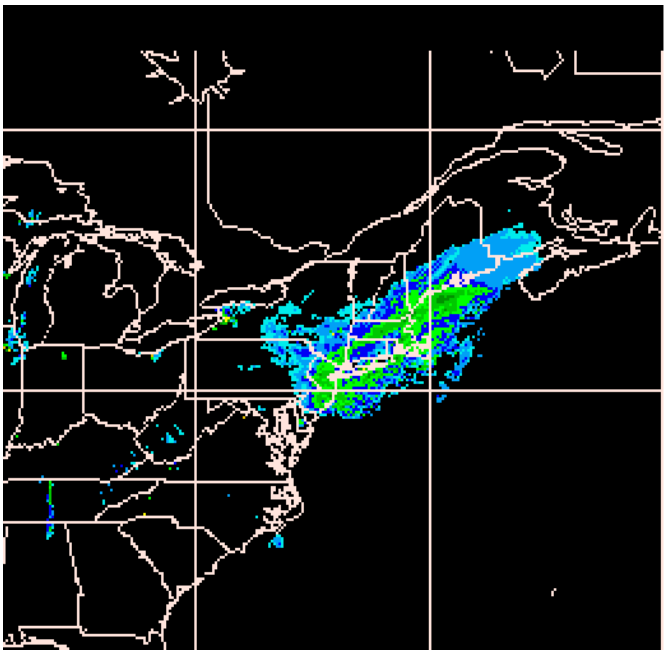

Figure 8. A 2-km resolution WSR-88D mosaic of 0.5° reflectivity (CONUS-scale), valid at 1200 UTC, Jan. 23, 2005.

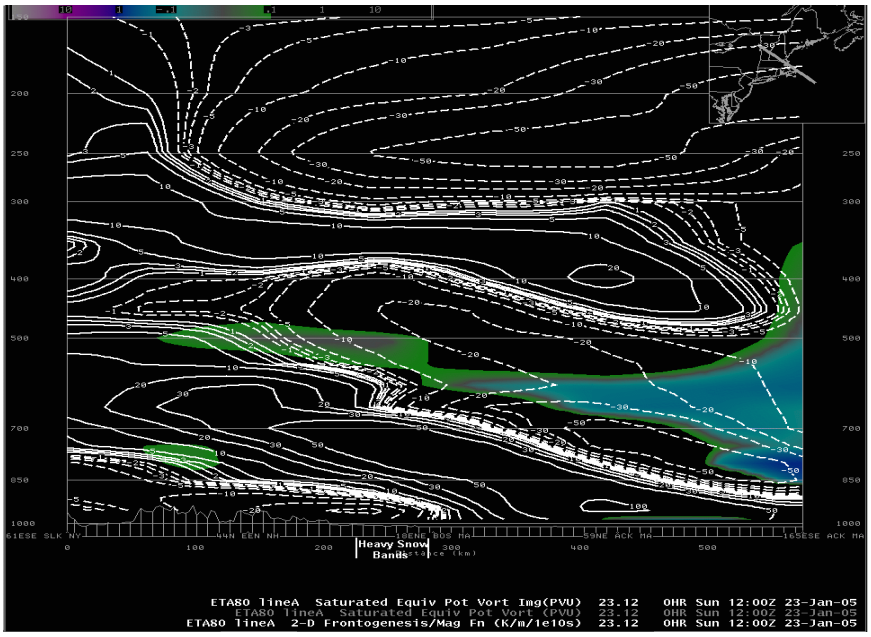

Figure 9. NAM initialized cross-section of 2-D frontogenesis (solid white, °K (100 km)$^{-1}$ (3h)$^{-1}$) and saturated EPV (negative and weakly positive (0.0 to 0.1 PVU) values shaded, 10^{-7} °K (Pa s)$^{-1}$), valid at 12 UTC, Jan. 23, 2005. The cross-sectional axis was drawn from southeast of Nantucket, Massachusetts to Vermont. The approximate location of heavy snow bands are noted along the x-axis.

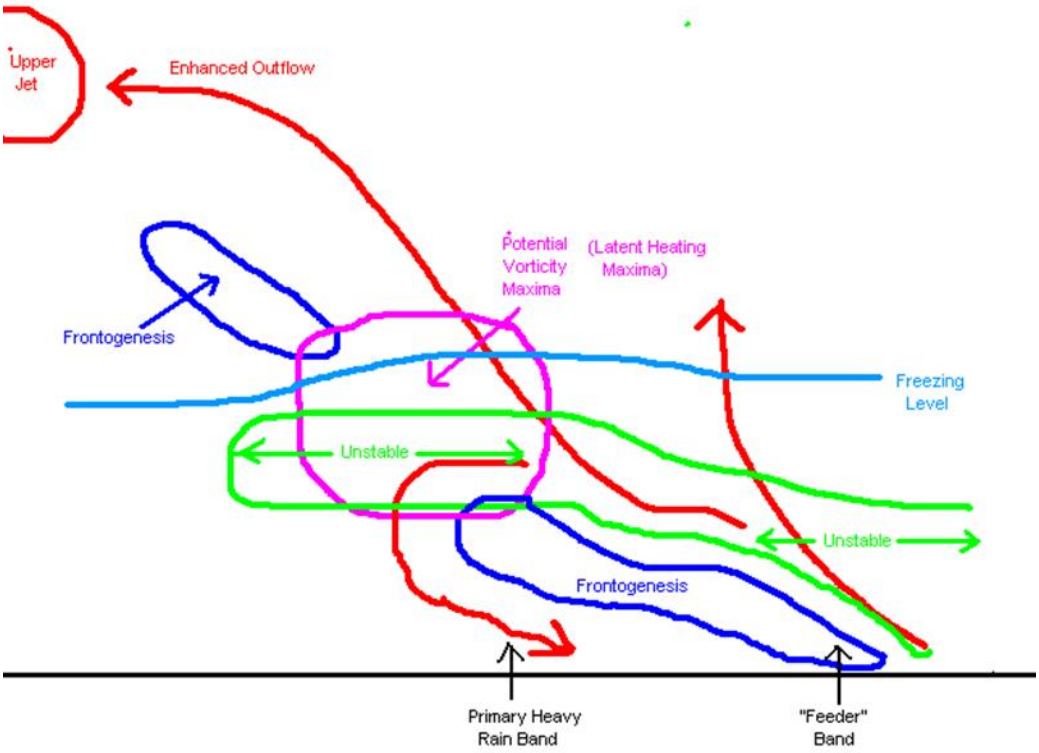

Figure 10. Three-dimensional schematic of primary atmospheric ingredients that contributed to heavy stratiform rainfall, while Ivan and Frances were undergoing their extra-tropical transitions.